Available online at www.sciencedirect.com
ScienceDirect
Trans. Nonferrous Met. Soc. China 31(2021) 586−594
Transactions of Nonferrous Metals Society of China
www.tnmsc.cn

Mechanical and thermo-physical properties of rapidly solidified Al−50Si−Cu(Mg) alloys for thermal management application

Jun FANG, Yong-hui ZHONG, Ming-kuang XIA, Feng-wei ZHANG

The 43 Research Institute of China Electronic Technology Group Corporation, Hefei 230088, China

Received 20 April 2020; accepted 30 October 2020

Abstract: Al−high Si alloys were designed by the addition of Cu or Mg alloying elements to improve the mechanical properties. It is found that the addition of 1 wt.% Cu or 1 wt.% Mg as strengthening elements significantly improves the tensile strength by 27.2% and 24.5%, respectively. This phenomenon is attributed to the formation of uniformly dispersed fine particles (Al_2Cu and Mg_2Si secondary phases) in the Al matrix during hot press sintering of the rapidly solidified (gas atomization) powder. The thermal conductivity of the Al−50Si alloys is reduced with the addition of Cu or Mg, by only 7.3% and 6.8%, respectively. Therefore, the strength of the Al−50Si alloys is enhanced while maintaining their excellent thermo-physical properties by adding 1% Cu(Mg).

Key words: Al−50Si alloy; rapid solidification; thermal management material; mechanical property; thermo-physical property

1 Introduction

Al−Si alloys containing high Si contents, also called as Al−high Si alloys or Si_p/Al composites, exhibit an excellent combination of thermo-physical properties and mechanical properties, such as low density, excellent thermal conductivity, tailorable coefficient of thermal expansion, and high specific strength [1−4]. Additionally, Al−high Si alloys also have good plating ability and laser weldability. There characteristics make Al−high Si alloys attractive for electronic packaging applications in the field of thermal management, especially for chip boxes to protect electronic devices from outdoor environments [5].

It is well known that the properties of Al−high Si alloys are determined by the size, shape and distribution of Si phase, including primary Si and eutectic Si phase [6,7]. The application of ingot metallurgy (IM) Al−high Si alloys is highly limited by the formation of the coarse and irregular primary Si phase as well as the lager needle-like eutectic Si phase. These microstructural characteristics lead to stress concentration and are detrimental to the mechanical properties and laser weldability. Therefore, a simple and effective route to refine and modify the Si phase is essential to the wide application of Al−high Si alloys.

Lots of methods have been employed in the preparation of Al−high Si alloys, such as semi-solid forming [8], melt infiltration [9], ingot metallurgy with modifiers [10,11], powder metallurgy [12], rapid solidification [13] and the recently developed selective laser melting [14,15]. According to the literatures, the rapid solidification route is more feasible for mass manufacturing of Al−high Si alloys for thermal management due to the advantages of high efficiency, remarkable refinement effect and ingots with large size. JIA et al [13] reported that the spray deposited Al−50Si alloy can be completely densified by hot isostatic

Corresponding author: Jun FANG; Tel: +86-551-65748315; E-mail: fangjun960@163.com
DOI: 10.1016/S1003-6326(21)65521-8

pressing (HIP) at 570 °C. Al alloys with Si content of 22%−50% were prepared by gas atomization followed by hot pressing, and near fully dense microstructure and excellent properties were obtained [16]. Al−30Si alloy prepared by spray deposition can also be densified by hot pressing, and a continuous network of globular Si phase and an interpenetrating Al matrix were achieved [17].

The Al−50Si alloy is widely used as electronic packaging boxes, which has a high volume fraction of Si and approximately pure Al matrix. However, its strength should be improved in order to expand its application [5]. The previous works of Al−high Si alloys for thermal management have been focused on the manufacturing technologies, parameters, and the subsequent properties. Generally, the properties of ingot metallurgy Al−high Si alloys can be modified through alloying, such as the A356, A380, and A390 alloys [18]. BEFFORT et al [19] reported that mechanical properties of the squeeze cast 60vol.%SiC_p/Al composites were also highly determined by the Zn, Cu and Mg elements in the Al matrix. However, less attention has been paid to the alloy composition and the relationship between microstructural evolution and properties of the Al−50Si alloy.

Accordingly, in this work, Al−50Si, Al−50Si−1Cu and Al−50Si−1Mg alloys for electronic packaging in thermal management were successfully fabricated by rapid solidification (gas atomization) and powder metallurgy (hot pressing) route, and the microstructural characteristics, mechanical properties (tensile and bending strength) and thermo-physical properties were studied. Comparisons between the effect of Cu and Mg addition on the Al−50Si alloys were analyzed based on the microstructural observations and macro-property tests.

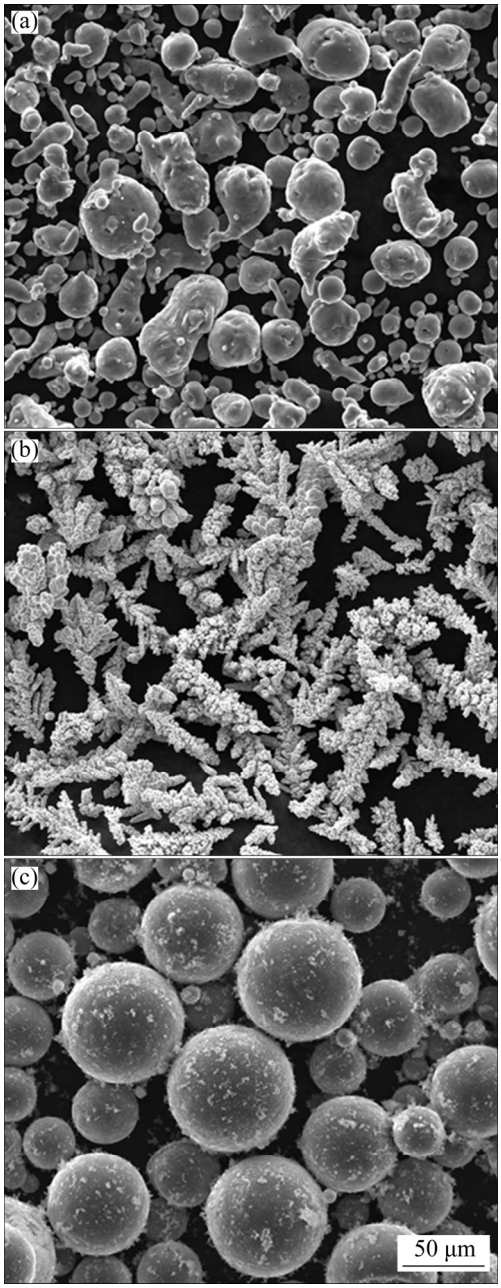

Fig. 1 SEM morphologies of gas-atomized Al−50Si pre-alloy powder (a), electrolytic Cu powder (b) and inert gas-atomized Mg powder (c) with different shapes

2 Experimental

Polycrystalline pure Si (99.9%, all the alloy compositions are in mass fraction unless otherwise mentioned) and pure Al (99.95%) were inductively melted at approximately 1250 °C. Then, Al−50Si pre-alloy powder was fabricated through a nitrogen gas atomization process, and the morphology of the powder particles is shown in Fig. 1(a). After mechanical sieving, the Al−50Si pre-alloy powder with particle size less than 74 μm was mixed with 1 wt.% electrolytic Cu powder and 1 wt.% inert gas-atomized Mg powder, respectively. Mechanical mixing was applied for 6 h in the atmosphere of Ar with the mass ratio of ball to powder of 4:1. The Cu and Mg powders having dendritic and spherical shapes are displayed in Figs. 1(b) and 1(c), respectively. The mixed powder was cold compacted at 300 MPa and hold for 20 s, and billets with relative density of approximately 78% were obtained. Hot press sintering was employed on the cold compacted billets and held at 560 °C for

60 min at 45 MPa. Finally, the samples with dimensions of *d*50 mm × 10 mm were obtained. The hot-pressed alloys were solid solutionized at 500 °C for 4 h and then aged at 160 °C for 24 h. Details of the fabrication process is reported in the previous work [16].

Chemical compositions of the as-fabricated Al−50Si−X (X=0, Cu, and Mg) alloys were detected using an inductively coupled plasma optical emission spectrometer (IC-OES), and the results are illustrated in Table 1. Morphologies of the Al−50Si pre-alloy powders, Cu powder and Mg powder were detected using a scanning electron microscope (SEM, Quanta−200). Hot-pressed samples for microstructural characterization were cut, ground, polished, and etched with Keller's reagent. Field emission scanning electron microscope (FESEM, Sirion 200) equipped with an energy dispersive spectroscopy (EDS) detector was used in the observation of microstructural details. The sizes of Si phase and secondary phases were measured using ImageJ software. The phases present in the Al−high Si alloys were further analyzed using X-ray diffraction (XRD) at a scanning angle of 25°−80°.

The room temperature tensile and three-point bending tests of samples were carried out on an electronic universal material testing machine (MTS 850). The tensile specimens were made into a dumbbell shape according to the standard GB T228—2010 with a gauge diameter of 6 mm. The dimensions of the three-point bending specimen are 3 mm × 10 mm × 50 mm. The tensile fractured surfaces of the specimens were observed using SEM. The Brinell hardness test of the alloy was performed at a load of 7.35 kN for 30 s on the polished samples. All the tensile and bending tests were repeated three times to obtain good reproducibility of data.

Under the argon atmosphere, coefficient of thermal expansion of the Al−50Si−X alloys was measured in the temperature range of 25−300 °C using laser flash and calorimetric methods (NETZSCH LFA427/3/G). The sample has a size of 20 mm × 5 mm × 5 mm and was required to be parallel and smooth at both ends. Thermal conductivity of the three kinds of alloys was performed on cylindrical slice specimens with dimensions of *d*10 mm × 3 mm using NETZSCH DIL 402 C. Density of the alloys was measured by Archimedes method using a balance with the accuracy of 0.1 mg.

3 Results

3.1 Microstructural characteristics

Typical microstructures of the as-atomized Al−50Si pre-alloy powder and the hot-pressed Al−50Si−X alloys are shown in Fig. 2. It can be seen from Fig. 2(a) that the primary Si phase is highly refined to have a block-like morphology due to the large solidification rate and undercooling nature of gas atomization. The eutectic Si phase is also refined remarkably and its shape changes from needle-like with large aspect ratio in the as-cast alloy to bar-like with a low aspect ratio in the as-atomized powder. However, the primary Si seems to distribute mostly at the periphery of powder particles owing to the solidification sequence [20].

After hot press, the gas-atomized Al−50Si pre-alloy powder is well densified and a pore-free microstructure is obtained, as shown in Figs. 2(b−d). High density of defects, such as pores and cracks were observed in the Al−50Si alloy prepared by ingot metallurgy [21]. Consequently, the measured density of the hot-pressed samples is near to the theoretical value. As the density of Cu (8.9 g/cm^3) is higher than that of Al (2.7 g/cm^3) while the density of Mg (1.7 g/cm^3) is lower than that of Al, the addition of Cu or Mg leads to a slight variation of density in the Al−50Si−X alloys.

Table 1 Compositions of rapidly solidified (gas-atomized) and hot-pressed Al−50Si−X alloys measured by ICP-OES (wt.%)

Material	Si	Mg	Cu	Zn	Fe	Mn	Ti	Al
Al−50Si	50.5	<0.01	<0.01	<0.01	0.04	0.02	<0.01	Bal.
Al−50Si−1Cu	50.3	0.05	1.03	<0.01	0.03	0.01	<0.01	Bal.
Al−50Si−1Mg	49.7	1.03	0.02	<0.01	0.05	0.01	<0.01	Bal.

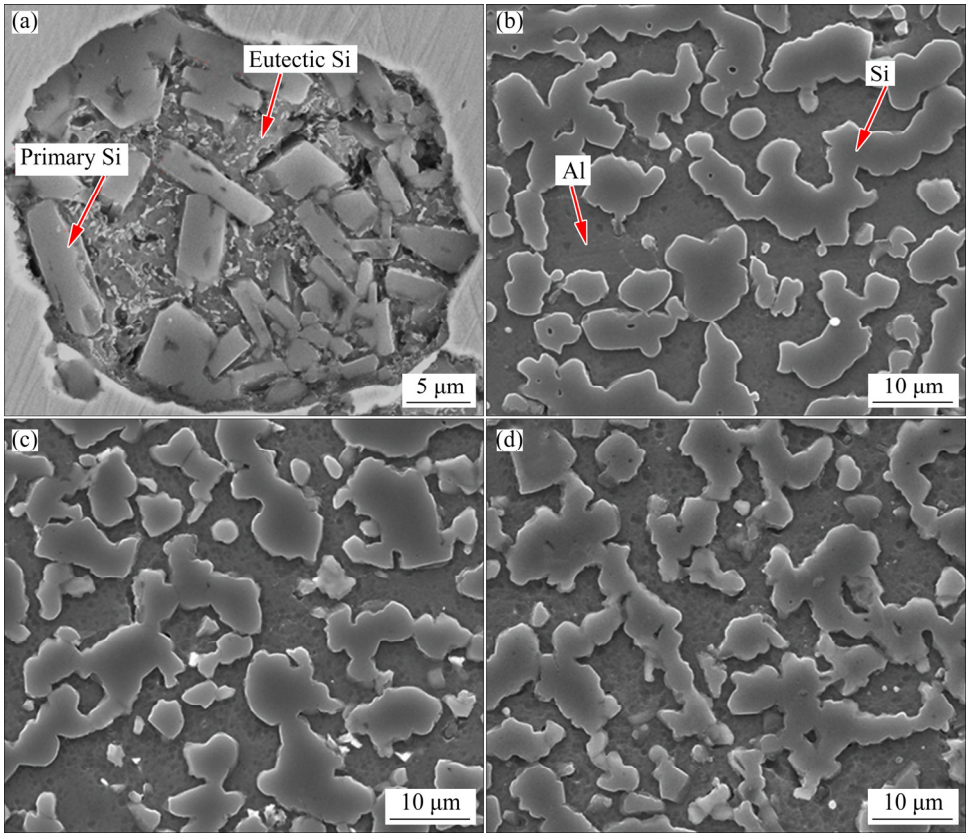

Fig. 2 SEM morphologies of gas-atomized Al−50Si pre-alloy powder (a) and as-fabricated Al−50Si alloy (b), Al−50Si−1Cu alloy (c) and Al−50Si−1Mg alloy (d) having similar characteristics of Si phase

It is seen that a semi-continuous network structure with smooth surface of the Si phase is formed in the Al matrix, as seen in Figs. 2(b−d). The distribution of Si phase is quite homogeneous as compared with that of the as-atomized powder. Such characteristics of Si phase are highly different from those of the as-cast Al−high Si alloys which have coarse and irregular (bar-like, plate-like, star-like, etc) primary Si with sharp corners as well as needle-like eutectic Si with a large aspect ratio [11,21]. Furthermore, it is interesting to find that the eutectic Si is completely absent in the hot-pressed samples due to the diffusion-controlled growth of Si phase and the Si−Si phase clustering in the solid-state sintering. There is no obvious change of the Si phase in the fabricated Al−50Si alloys with and without Cu(Mg) addition besides a little lower degree of the semi-continuous structure.

X-ray diffractions were performed to detect the phases presented in the hot-pressed Al−50Si−X alloys, and the results are displayed in Fig. 3. It is seen that the diffraction peaks of α(Al) and Si phase are clearly observed in the samples. With the addition of Cu or Mg, small amounts of Al_2Cu and

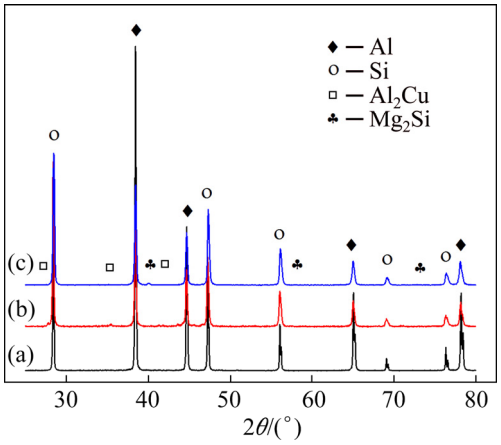

Fig. 3 XRD patterns of as-fabricated Al−50Si−X alloys showing Al_2Cu and Mg_2Si secondary phases formed in Al−50Si−Cu/(Mg) alloys: (a) Al−50Si; (b) Al−50Si−1Cu; (c) Al−50Si−1Mg

Mg_2Si secondary phases are formed in the Al−50Si−Cu(Mg) alloys. It is noted that, different from the Al−50Si−1Cu alloy, no AlMg secondary phases are formed in the Al−50Si−1Mg alloy. However, as the content of Cu or Mg is only 1%, the diffraction peaks of the Al_2Cu and Mg_2Si phases are not remarkable.

To further investigate the secondary phases formed in the Al−50Si−Cu(Mg) alloys, magnified SEM observations were conducted and the results are shown in Fig. 4. Other than the large Si particles, small needle-like Al_2Cu phase and bar-like Mg_2Si phase are present in the Al−50Si−Cu(Mg) alloys. This result is in consistent with the XRD patterns presented in Fig. 3. Although the average sizes of the Al_2Cu and Mg_2Si secondary phases are less than 1 μm, most of the Mg_2Si phase is larger than the Al_2Cu phase. Additionally, most of the Al_2Cu phases are dispersed in the center of the Al matrix. However, the Mg_2Si phase seems to distribute mostly near the surface of Si particles. This phenomenon can be attributed to the larger diffusion rate and supersaturation of Mg than those of Si in the Al matrix.

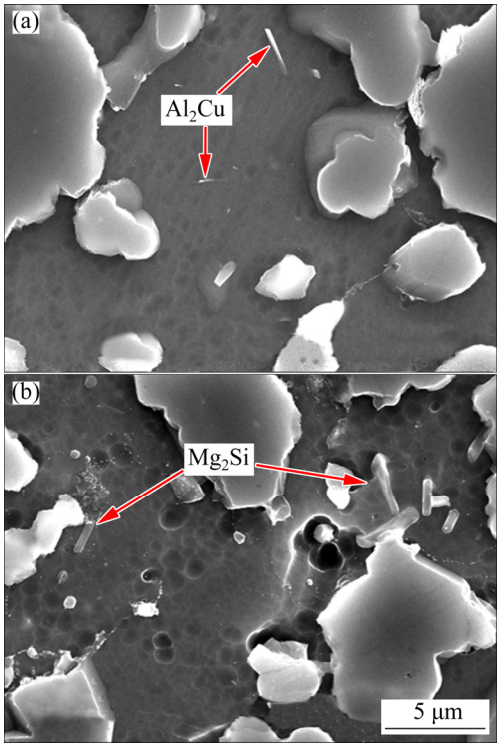

Fig. 4 SEM morphologies and distribution of Al_2Cu (a) and Mg_2Si (b) secondary phases present in Al−50Si−Cu(Mg) alloys

3.2 Mechanical properties

The room temperature tensile tests were performed on the hot-pressed Al−50Si alloys with and without Cu(Mg) addition, and the tensile curves are depicted in Fig. 5. The stress−strain response of the Al−50Si alloy is different from that containing Cu and Mg. A very slight plastic deformation of approximately 0.5% strain is observed in the Al−50Si alloy. Remarkably enhanced ultimate tensile strength (UTS) is achieved in the Al−50Si−1Cu and Al−50Si−1Mg alloys. The plastic behavior is less evident, approximately 0.3% strain to fracture, with the addition of Cu or Mg. This phenomenon indicates that the addition of Cu(Mg) is beneficial to improving the strength of Al−50Si alloy but detrimental to the plasticity of the alloy. Additionally, the slope of the tensile stress−strain response of the Cu(Mg)-contained alloys becomes flatter and higher than that of the Al−50Si alloy, suggesting that the addition of Cu(Mg) also enhances the elastic modulus of the alloy.

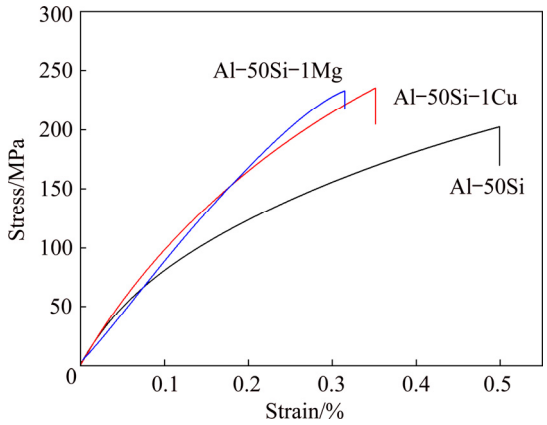

Fig. 5 Tensile stress−strain response of rapidly solidified Al−50Si−X alloys at room temperature

Average values of the tensile strength, bending strength and hardness of the Al−50Si−X alloys were obtained from five parallel tests, and the results are shown in Fig. 6. The strength of the Al−50Si alloy is significantly improved with the addition of Cu(Mg). Compared with the reference sample, the addition of 1% Cu raises the tensile and bending strength from 185.7 and 288.6 MPa to 236.2 and 390.5 MPa, with increments of 27.2% and 35.3%, respectively. Similarly, the addition of 1% Mg results in an enhancement of tensile and bending strength by 24.5% and 29.0%, respectively. At the same time, the addition of alloying elements also increases the hardness of the Al matrix. From Fig. 6, it is also found that the strengthening effect of Cu is slightly higher than that of Mg. This phenomenon can be attributed to the fine and homogeneous distribution of the Al_2Cu secondary phase at the center of the Al matrix. Additionally, according to the image analysis from SEM results, the average size of Al_2Cu phase is a little smaller

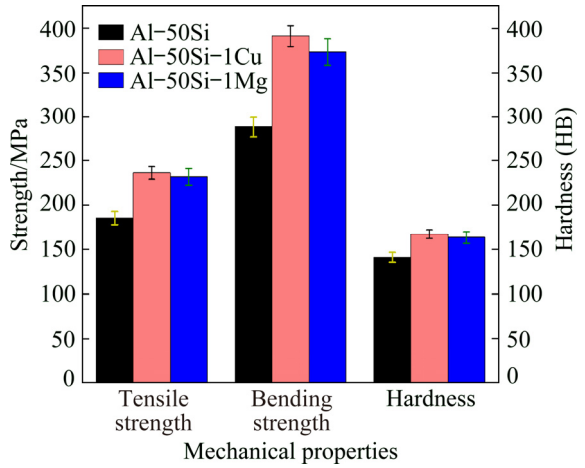

Fig. 6 Tensile strength, bending strength and hardness of rapidly solidified Al−50Si−X alloys

than that of the Mg_2Si phase, which may also contribute to the higher strength of the Al−50Si−1Cu alloy.

Tensile fractured morphologies of Al−50Si−X alloys are displayed in Fig. 7. All samples show a clear brittle fracture feature. It is seen that the fracture planes of the alloys are vertical to the tensile direction and no visible macro-ductility fracture is observed. As seen from Fig. 7(a), the crack source of the alloy with rather flat morphology is clearly observed. The crack progresses rapidly in a linear way through the sample when external pressure is applied. Figures 7(b−d) show that the Al matrix fractures by ductile rupture with tearing ridge while the Si phase fractures by cleavage surface. As there is a high volume fracture of Si phase (approximately 53.7%) with semi-continuous structure, the Si particle dominated brittle fracture is the main mode of the Al−50Si alloys. The previous observation suggests that the crack tip moves through brittle fracture of the Si particles and finishes by ductile fracture of the Al matrix [22]. Generally, metal matrix composites (MMCs) reinforced with high volume of reinforcement fracture in such particle dominated

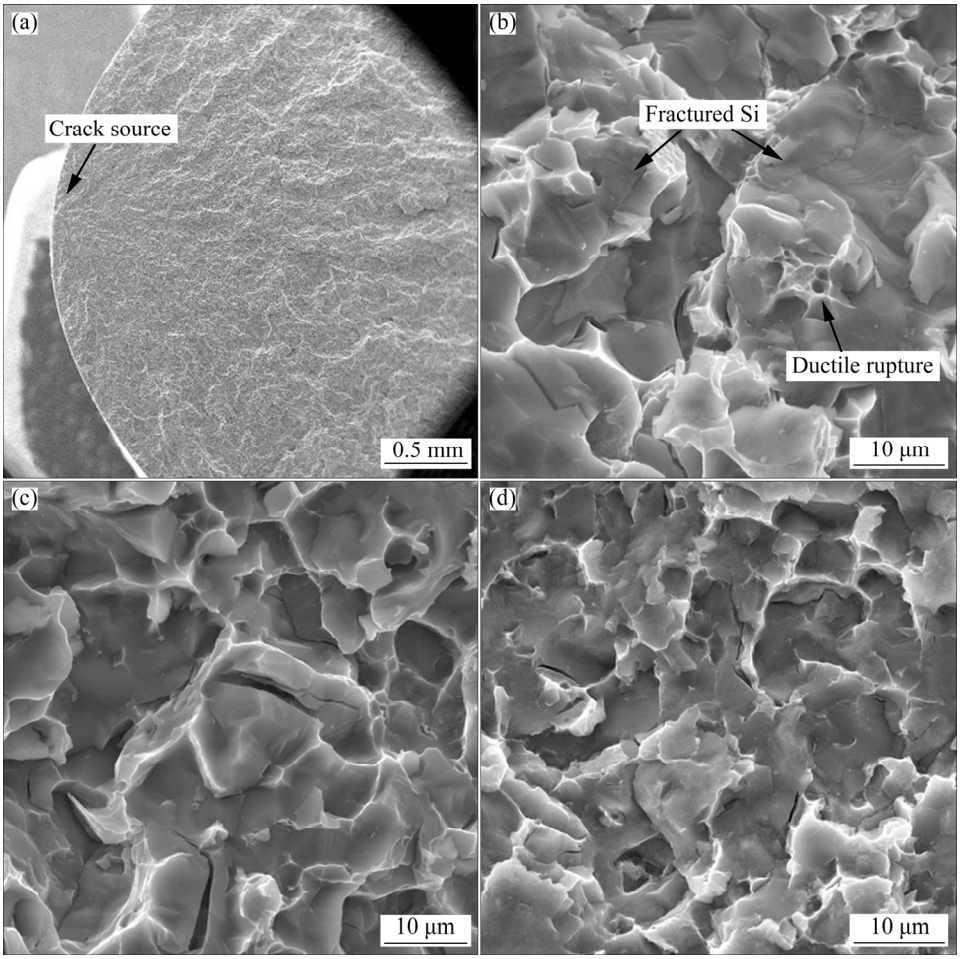

Fig. 7 Low magnification micrograph showing crack source of Al−50Si alloy (a) and high magnification micrographs of Al−50Si alloy (b), Al−50Si−1Cu alloy (c) and Al−50Si−1Mg alloy (d)

mode [23,24]. Additionally, dimples with small size are observed in the alloys due to the refined microstructure as a result of rapid solidification and solid-state sintering. However, three kinds of alloys show typical brittle fracture, and the difference among fractured morphologies is less visible.

3.3 Thermo-physical properties

Variations of coefficient of thermal expansion (CTE) of the Al−50Si−X alloys as a function of temperature in the range of 25−300 °C are shown in Fig. 8. It is observed that the coefficient of thermal expansion increases linearly with the increase of testing temperature. The Al−high Si alloys can be regarded as Si particle reinforced Al matrix composites (Si_p/Al) and the coefficient of thermal expansion of the alloy is mainly determined by the properties of the Al matrix and Si phase and the volume fraction of the Si phase according to the rule of mixture (ROM). As seen from Fig. 2, there is little deviation of the volume fraction, size, and morphology of Si phase. Consequently, the coefficients of thermal expansion of the Al−50Si−X alloys are determined mainly by the properties of Al matrix. Owing to the presence of Al_2Cu and Mg_2Si secondary phase having lower coefficient of thermal expansion, the total thermal expansion of Al−50Si alloys is reduced. JIA et al [13] reported that no plastic deformation occurs in the Al matrix at low temperatures. The expansion of the alloys is caused by the combined expansion of the Al matrix and Si phase and results in the linearly increased coefficient of thermal expansion with increasing temperature.

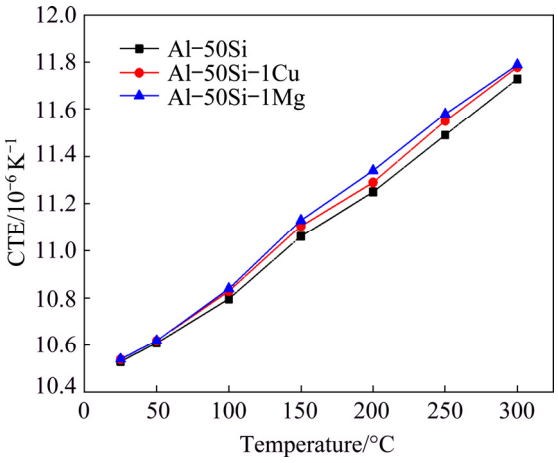

Fig. 8 Coefficient of thermal expansion of rapidly solidified Al−50Si−X alloys in temperature range of 25−300 °C

Thermal conductivity of the Al−50Si−X alloys is illustrated in Fig. 9. Owing to the rapid solidification nature of gas atomization and the diffusion-controlled growth of Si phase during hot pressing, the Si phase has a semi-continuous structure with smooth surface, which contributes to the excellent thermal conductivity of the Al−50Si alloy, 146.2 $W \cdot m^{-1} \cdot K^{-1}$. At the same time, Si has low solid solubility in the Al matrix with equilibrium state, and a near pure Al matrix after hot pressing may also help for achieving high thermal conductivity of the alloy. However, the formation of the Al_2Cu and Mg_2Si secondary phases in the Al−50Si−Cu(Mg) alloys has a scattering effect on the free electron motion and hinders the thermal conduction [25]. Consequently, the thermal conductivities of the Al−50Si alloy containing 1% Cu and 1% Mg are reduced by 7.3% and 6.8%, respectively. In comparison with the exceptionally improved strength of the Al−50Si alloy, this reduction of thermal conductivity is within the acceptable limit (≥120 $W \cdot m^{-1} \cdot K^{-1}$).

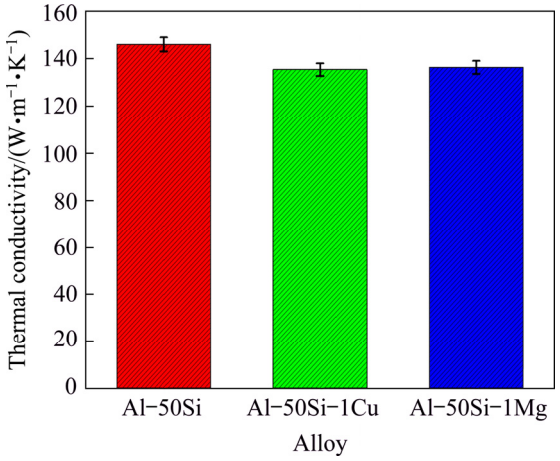

Fig. 9 Thermal conductivity of rapidly solidified and hot-pressed Al−50Si−X alloys at room temperature

4 Conclusions

(1) Gas atomization endows the pre-alloyed Al−50Si alloy powder with highly refined primary and eutectic Si phase, and in combination with the subsequent solid-state hot-pressing, the Si phase with semi-continuous network structure is obtained. By adding 1% Cu or 1% Mg, Al_2Cu or Mg_2Si secondary phases are observed, respectively, but the influence on the Si phase characteristics is limited.

(2) Tensile strength, bending strength and hardness of the Al−50Si alloys are significantly

improved with the addition of Cu or Mg, respectively, which is attributed to the strengthening effect of the fine secondary phases. The effect of Cu on mechanical properties is more remarkable compared with that of Mg. All the Al−50Si−X alloys show typical brittle fracture features having a clear cleavage surface.

(3) The addition of Cu(Mg) is helpful for reducing the coefficient of thermal expansion of the Al−50Si−X alloys, but detrimental to the thermal conductivity. However, negligible difference in thermo-physical properties is observed in the Al−50Si−Cu(Mg) alloys.

References

[1] HOGG S C, LAMBOURNE A, OGILVY A, GRANT P S, Microstructural characterisation of spray formed Si−30Al for thermal management applications [J]. Scripta Materialia, 2006, 55(1): 111−114.

[2] KIMURA T, NAKAMOTO T, MIZUNO M, ARAKI H. Effect of silicon content on densification, mechanical and thermal properties of Al−*x*Si binary alloys fabricated using selective laser melting [J]. Materials Science and Engineering A, 2017, 682: 593−602.

[3] ZHANG Wen-long, DING Dong-yan, GAO Ping. High volume fraction Si particle-reinforced aluminium matrix composites fabricated by a filtration squeeze casting route [J]. Materials & Design, 2016, 90: 834−838.

[4] WANG Qian, ZHU Lin, CHEN Xiao-guang, YAN Jiu-chun, XIE Rui-shan, LI Pei-hao, WANG Zhi-hua, WANG Zhi-qi, LI Yun-tao, ZHOU Xiao-yu. Si particulate-reinforced ZnAl based composites joints of hypereutectic Al50Si alloys by ultrasonic-assisted soldering [J]. Materials & Design, 2016, 107: 41−46.

[5] MAUDUIT D, DUSSERRE G, CUTARD T. Probabilistic rupture analysis of a brittle spray deposited Si−Al alloy under thermal gradient: Characterization and thermoelastic sizing guidelines [J]. Materials & Design, 2016, 95: 414−421.

[6] CHEN Xu, ZHONG Yun-bo, ZHENG Tian-xiang, SHEN Zhe, WANG Jiang, FAN Li-jun, ZHAI Yong, PENG Ming-hu, ZHOU Bang-fei, REN Wei-li, LEI Zuo-sheng, REN Zhong-ming, HE Qiong. Refinement of primary Si in the bulk solidified Al−20wt.%Si alloy assisting by high static magnetic field and phosphorus addition [J]. Journal of Alloys and Compounds, 2017, 714: 39−46.

[7] WANKHEDE D M, NARKHEDE B E, MAHAJAN S K, CHOUDHARI C M. Influence of pouring temperature and external chills on mechanical properties of aluminum silicon alloy castings [J]. Materials Today: Proceedings, 2018, 5(9): 17627−17635.

[8] WARD P J, ATKINSON H V, ANDERSON P R G, ELIAS L G, GARCIA B, KAHLEN L, RODRIGUEZ-IBABE J M. Semi-solid processing of novel MMCs based on hypereutectic aluminium-silicon alloys [J]. Acta Materialia, 1996, 44(5): 1717−1727.

[9] CHEN Yu-yong, CHUNG D D L. Silicon-aluminium network composites fabricated by liquid metal infiltration [J]. Journal of Materials Science, 1994, 29(23): 6069−6075.

[10] RAGHUKIRAN N, KUMAR R. Effect of scandium addition on the microstructure, mechanical and wear properties of the spray formed hypereutectic aluminum−silicon alloys [J]. Materials Science and Engineering A, 2015, 641: 138−147.

[11] YU Wen-hui, ZHANG Yong, YAN Ting-liang, LIU Yue, JIANG Ao-lei, ZHENG Hong-liang, TIAN Xue-lei. Enhanced nucleation of primary silicon in Al−20wt.%Si alloy with Ni−Si inoculation [J]. Journal of Alloys and Compounds, 2017, 693: 303−307.

[12] LIU Y Q, WEI S H, FAN J Z, MA Z L, ZUO T. Mechanical properties of a low thermal-expansion aluminum/silicon composite produced by powder metallurgy [J]. Journal of Materials Science & Technology, 2014, 30(4): 417−422.

[13] JIA Yan-dong, CAO Fu-yang, SCUDINO S, MA Pan, LI Hai-chao, YU Lei, ECKERT J, SUN Jian-fei. Microstructure and thermal expansion behavior of spray-deposited Al−50Si [J]. Materials & Design, 2014, 57: 585−591.

[14] JIA Qing-bo, ROMETSCH P, KURNSTINER P, CHAO Qi, HUANG Ai-jun, WEYLAND M, BOURGEOIS L, WU Xin-hua. Selective laser melting of a high strength Al−Mn−Sc alloy: Alloy design and strengthening mechanisms [J]. Acta Materialia, 2019, 171: 108−118.

[15] KANG Nan, CODDET P, LIAO Han-lin, CODDET C. Macrosegregation mechanism of primary silicon phase in selective laser melting hypereutectic Al−high Si alloy [J]. Journal of Alloys and Compounds, 2016, 662: 259−262.

[16] CAI Zhi-yong, ZHANG Chun, WANG Ri-chu, PENG Chao-qun, QIU Ke, FENG Yan. Preparation of Al−Si alloys by a rapid solidification and powder metallurgy route [J]. Materials & Design, 2015, 87: 996−1002.

[17] WANG Feng, XIONG Bai-qing, ZHANG Yong-an, ZHU Bao-hong, LIU Hong-wei, WEI Yan-guang. Microstructure, thermo-physical and mechanical properties of spray-deposited Si−30Al alloy for electronic packaging application [J]. Materials Characterization, 2018, 59(10): 1455−1457.

[18] DAMAVANDI E, NOUROUZI S, RABIEE S M, JAMAATI R. Effect of ECAP on microstructure and tensile properties of A390 aluminum alloy [J]. Transactions of Nonferrous Metals Society of China, 2019, 29(5): 931−940.

[19] BEFFORT O, LONG Si-yuan, CAYRON C, KUEBLER J, BUFFAT P A. Alloying effects on microstructure and mechanical properties of high volume fraction SiC particle reinforced Al-MMCs made by squeeze casting infiltration [J]. Composites Science and Technology, 2007, 67(3): 737−745.

[20] KALAY Y E, CHUMBLEY L S, ANDERSON I E, NAPOLITANO R E. Characterization of hypereutectic Al−Si powders solidified under far-from equilibrium conditions [J]. Metallurgical and Materials Transactions A, 2007, 38(7): 1452−1457.

[21] CAO Fu-yang, JIA Yan-dong, PRASHANTH K G, MA Pan, LIU Jing-shun, SCUDINO S, HUANG Feng, ECKERT J, SUN Jian-fei. Evolution of microstructure and mechanical properties of as-cast Al−50Si alloy due to heat treatment and P modifier content [J]. Materials & Design, 2015, 74: 150−156.

[22] CAI Zhi-yong, ZHANG Chun, WANG Ri-chu, PENG Chao-qun, WU Xiang. Effect of copper content on microstructure and mechanical properties of Al/Si_p composites consolidated by liquid phase hot pressing [J]. Materials & Design, 2016, 110: 10−17.

[23] ZHANG Qi-guo, ZHANG Hong-xiang, GU Ming-yuan, JIN Yan-ping. Studies on the fracture and flexural strength of Al/Si_p composite [J]. Materials Letters, 2004, 58: 3545−3550.

[24] BUFFIERE J Y, MAIRE E, VERDU C, CLOETENS P, PATEYRON M, PEIX G, BARUCHEL J. Damage assessment in an Al/SiC composite during monotonic tensile tests using synchrotron X-ray microtomography [J]. Materials Science and Engineering A, 1997, 234−236: 633−635.

[25] BLANK M, SCHNEIDER G, ORDONEZ-MIRANDA J, WEBER L. Role of the electron-phonon coupling on the thermal boundary conductance of metal/diamond interfaces with nanometric interlayers [J]. Journal of Applied Physics, 2019, 126: 165302.

热管理用快速凝固 Al−50Si−Cu(Mg)合金的力学和热物理性能

方 军，钟永辉，夏明旷，张凤伟

中国电子科技集团第四十三所，合肥 230088

摘 要：通过加入 Cu 或 Mg 合金元素提高高硅铝合金的力学性能。结果表明，加入 1% Cu 或 1% Mg(质量分数)可分别将抗拉强度提高 27.2%和 24.5%，这是由于快速凝固(气体雾化)粉末在热压烧结过程中，Al 基体中形成均匀分散的细小颗粒(Al_2Cu 和 Mg_2Si 第二相)。添加 Cu 或 Mg 仅降低 Al−50Si 合金的热导率 7.3%和 6.8%。因此，通过添加 1% Cu(Mg)，可以在保持 Al−50Si 合金优异热物理性能的同时提高其强度。

关键词：Al−50Si 合金；快速凝固；热管理材料；力学性能；热物理性能

(Edited by Bing YANG)